JOC Article
pubs.acs.org/joc

$TiCl_4$-Promoted Baylis−Hillman Reaction: Mechanistic Rationale toward Product Distribution and Stereoselectivity

Chandan Patel and Raghavan B. Sunoj*

Department of Chemistry, Indian Institute of Technology Bombay Powai, Mumbai 400076

sunoj@chem.iitb.ac.in

Received October 2, 2009

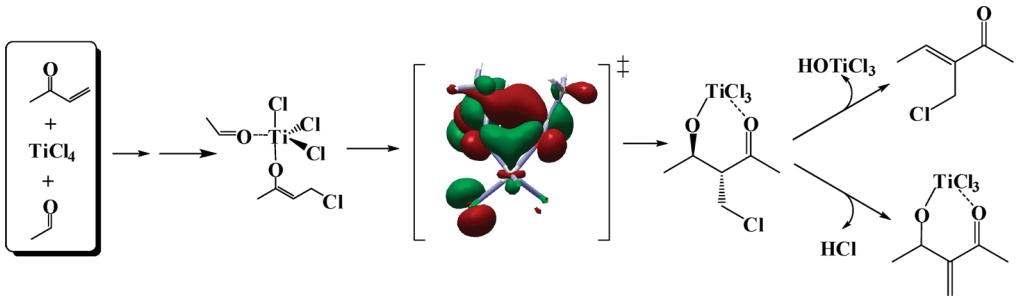

The mechanism of $TiCl_4$-promoted Baylis−Hillman reaction between methyl vinyl ketone (MVK) and acetaldehyde, in the absence of any base, is studied using the mPW1K density functional theory. The study focuses on several mechanistic intricacies as well as selectivity issues at each step of the reaction. The minimum energy pathway for this reaction involves three major steps such as a chloride transfer resulting in a chloro-enolate, titanium-mediated aldol reaction, and elimination of HCl or $HOTiCl_3$. Both *s-cis* and *s-trans* conformers of MVK are considered along with various modes of chloride transfer involving different complexes between $TiCl_4$, aldehyde, and MVK. Chloride transfer is found to be kinetically more favored for *s-cis*-MVK than for *s-trans*-MVK. The diastereoselectivity in the next step, i.e., Ti-mediated aldol reaction between the enolate and aldehyde, is found to be dependent on the geometry of the enolate, wherein *anti* and *syn* BH products are predicted for *Z* and *E* enolates, respectively. An interesting secondary orbital interaction between the oxygen atoms of the enolate and aldehyde moieties in the transition states for the C−C bond formation is identified as one of the contributing factors toward the predicted diastereoselectivity in the formation of the α-chloromethyl aldol product (**P2**). It has earlier been reported that under different experimental conditions, any of the three products such as (i) a normal BH product (**P1**), (ii) 2-(chloromethyl)vinyl ketones (**P3**), and (iii) α-chloro methyl aldol could be generated (Scheme 1). The present study offers valuable insights toward rationalizing the observed product distribution as well as diastereoselectivity in $TiCl_4$-promoted BH reaction under base-free conditions. The computed energetics indicate that when MVK is employed as the Michael acceptor, the formation of 2-(choromethyl)vinyl ketone is the preferred product rather than the corresponding normal BH product, consistent with the known experimental reports.

Introduction

Over the years, the Baylis−Hillman (BH) reaction has become one of the most popular methods toward coupling activated olefins with a range of electrophilic acceptors, such as aldehydes.[1] As useful as it is in creating densely functionalized molecules, the BH reaction is also known to suffer from certain limitations. There have been a number of empirical approaches in circumventing the twin limitations of slow reaction rates and poor conversions.[2] The use of protic solvents or additives is now increasingly recognized as a simple and effective method for rate

(1) (a) Basavaiah, D.; Rao, A. J.; Satyanarayana, T. *Chem. Rev.* **2003**, *103*, 811. (b) Matsuya, Y.; Hayashi, K.; Nemoto, H. *J. Am. Chem. Soc.* **2003**, *125*, 646. (c) Shi, Y.-L. ; Shi, M. *Org. Lett.* **2005**, *7*, 3057. (d) Basavaiah, D.; Rao, K. V.; Reddy, R. J. *Chem. Soc. Rev.* **2007**, *36*, 1581.

(2) Some of the techniques that have been used to improve the rate of BH reaction include microwave irradiation, ultrasound, temperature, high pressure conditions, silica gel solid-phase medium, and so on.

DOI: 10.1021/jo902123x Published on Web 12/14/2009

SCHEME 1. Product Distribution for $TiCl_4$-Promoted BH Reaction between MVK and an Aldehyde under Different Reaction Conditions[a]

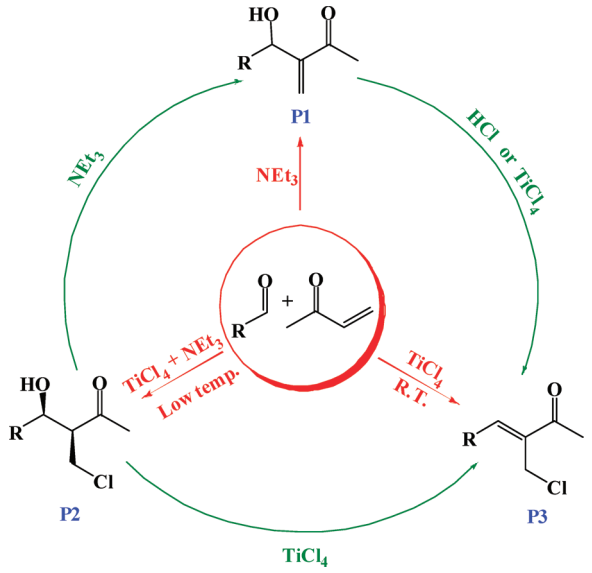

[a]The interconversion (shown in green) between the products might not lead to the same stereoisomer as shown.

enhancements.[3] In a very recent study, we have reported the mechanism of a tertiary amine-catalyzed BH reaction between methyl vinyl ketone (MVK) and benzaldehyde. It was proposed, in conjecture with the available experimental reports, that the key elementary steps involve the Michael addition of tertiary amine on MVK, addition of the zwitterionic intermediate thus generated to the aldehyde, intramolecular proton transfer, and lastly the elimination of the amine.[4] In another study, it was shown that the transition state for the C−C bond formation was much lower in energy than that of the proton transfer step, when explicit participation of co-catalyst/solvent molecule(s) is considered.[5] The rate enhancements in the BH reaction observed in the presence of hydrogen bond donors is usually attributed to the stabilization of the enolate intermediate and activation of the electrophile.[6]

Another commonly employed strategy to promote BH reaction involves the use of Lewis acids.[7,8] Lewis acid coordination could offer rate improvements through stabilization of the zwitterionic intermediates, as well as by imparting better electrophilicity on aldehydes. The use of Lewis acids has also been successful in asymmetric aldol reactions,[9] which constitutes a key step in BH reaction as well. Of particular relevance to the present study is the successful application of titanium(IV) complexes as Lewis acids in a variety of other asymmetric reactions including aldol, reduction of ketones, Diels−Alder, and carbonyl-ene reaction.[10]

A variety of other Lewis acids such as $AlCl_3$ and $ZnCl_2$ are also employed for BH reaction under base-free conditions.[11b] A wider range of Lewis acids, including $EtAlCl_3$, $BF_3 \cdot Et_2O$, $SnCl_4$, $SmCl_3$, etc., are reported to be useful under base-catalyzed BH reaction conditions.[11−14] However, $TiCl_4$ is known to be the most promising Lewis acid for this reaction owing to its potential in achieving high diastereoselectivity, enhanced rate, and versatility in terms of tolerance toward the presence of other Lewis bases and promoters, all these under ambient reaction conditions. More importantly, an interesting spectrum of products is observed in $TiCl_4$-mediated BH reaction under different reaction conditions. A summary of these possibilities is succinctly represented in Scheme 1. It is noticed that the normal BH product **P1** is obtained when only a tertiary amine or phosphine is employed as the catalyst.[1,11] However, $TiCl_4$ and Et_3N combination are known to produce either **P2** or **P3**, depending on the reaction temperature.[12,13] Interestingly, interconversion between these products is also established. For example, product **P2** (formed in $TiCl_4$−Lewis base promoted BH reaction) is known to transform into **P1** or **P3** by using excess of $TiCl_4$ or Et_3N.[14] In general, the diastereoselectivities for **P2** (*syn* diastereomer) and **P3** (Z configuration) are found to be good.

To the best of our knowledge, a comprehensive investigation focusing on the mechanism of Ti(IV)-promoted BH reaction is not reported as yet. A number of interesting questions on this important reaction thus continue to remain unanswered. It is equally important to note that the

(3) (a) Cai, J.; Zhou, Z.; Zhao, G.; Tang, C. *Org. Lett.* **2002**, *4*, 4723. (b) Faltin, C.; Fleming, E. M.; Connon, S. J. *J. Org. Chem.* **2004**, *69*, 6496.
(4) (a) Hill, J. S.; Isaacs, N. S. *J. Phys. Org. Chem.* **1990**, *3*, 285. (b) Roy, D.; Sunoj, R. B. *Org. Lett.* **2007**, *9*, 4873.
(5) (a) Aggarwal, V. K.; Fulford, S. Y.; Lloyd-Jones, G. C. *Angew. Chem., Int. Ed.* **2005**, *44*, 1706. (b) Robiette, R.; Aggarwal, V. K.; Harvey, J. N. *J. Am. Chem. Soc.* **2007**, *129*, 15513. (c) Roy, D.; Sunoj, R. B. *Chem.—Eur. J.* **2008**, *14*, 10530. (d) Roy, D.; Patel, C.; Sunoj, R. B. *J. Org. Chem.* **2009**, *74*, 3936.
(6) (a) Ameer, F.; Drewes, S. E.; Freese, S.; Kaye, P. T. *Synth. Commun.* **1988**, *18*, 495.
(7) (a) Kündig, E. P.; Xu, L. H.; Romanens, P.; Bernardinelli, G. *Tetrahedron Lett.* **1993**, *34*, 7049. (b) Aggarwal, V. K.; Mereu, A.; Tarver, G. J.; McCague, R. *J. Org. Chem.* **1998**, *63*, 7183. (c) Ono, M.; Nishimura, K.; Nagaoka, Y.; Tomioka, K. *Tetrahedron Lett.* **1999**, *40*, 1509. (d) Kawamura, M.; Kobayashi, S. *Tetrahedron Lett.* **1999**, *40*, 1539.
(8) Kataoka, T.; Iwama, T.; Tsujiyama, S.-I.; Iwamura, T.; Watanaba, S.-I. *Tetrahedron* **1998**, *54*, 11813.
(9) (a) March, J. *Advanced Organic Chemistry: Reactions, Mechanisms and Structure*; John Wiley & Sons: Singapore, 2003. (b) Parmee, E. R.; Tempkin, O.; Masamune, S.; Abiko, A. *J. Am. Chem. Soc.* **1991**, *113*, 9365. (c) Evans, D. A.; Tedrow, J. S.; Shaw, J. T.; Downey, C. W. *J. Am. Chem. Soc.* **2002**, *124*, 392. (d) Hamada, T.; Manabe, K.; Ishikawa, S.; Nagayama, S.; Shiro, M.; Kobayashi, S. *J. Am. Chem. Soc.* **2003**, *125*, 2989. (e) Avenoza, A.; Busto, J. H.; Canal, N.; Peregrina, J. M.; Pérez-Fernández, M. *Org. Lett.* **2005**, *7*, 3597. (f) Mlynarski, J.; Jankowska, J. *Adv. Synth. Catal.* **2005**, *347*, 521. (g) Geary, L. M.; Hultin, P. G. *Tetrahedron: Asymmetry* **2009**, *20*, 131.
(10) (a) Taniguchi, M.; Hino, T. *Tetrahedron Lett.* **1986**, *27*, 4767. (b) Sarko, C. R.; Guch, I. C.; DiMare, M. *J. Org. Chem.* **1994**, *59*, 705. (c) Terada, M.; Motoyama, Y.; Mikami, K. *Tetrahedron Lett.* **1994**, *35*, 6693. (d) Seebach, D.; Dahinden, R.; Marti, R. E.; Beck, A. K.; Plattner, D. A.; Kuhnle, F. N. M. *J. Org. Chem.* **1995**, *60*, 1788. (e) Ishimaru, K.; Monda, K.; Yamamoto, Y.; Akiba, K. *Tetrahedron* **1998**, *54*, 727.
(11) Product **P1** has also been observed in using $TiCl_4$/chalcogenide combination (e.g., SMe_2): (a) Kataoka, T.; Iwama, T.; Tsujiyama, S.-I. *Chem. Commun.* **1998**, *2*, 197 and for only $TiCl_4$-promoted BH reaction: (b) Li, G.; Wei, H. X.; Gao, J. J.; Caputo, T. D. *Tetrahedron Lett.*, **2000**, *41*, 1. However anti diastereomer of P2 was observed for N-acyl benzoaxazoline: (c) You, J.; Xu, J.; Verkade, J. G. *Angew. Chem., Int. Ed.* **2003**, *42*, 5054. (d) Kataoka, T.; Kinoshita, H. *Eur. J. Org. Chem.* **2005**, 45.
(12) Li, G.; Gao, J.; Wei, H. X.; Enright, M. *Org. Lett.* **2000**, *2*, 617.
(13) At lower temperatures (∼ −78 °C) product **P2** is exclusively found, whereas at higher temperatures (rt) only **P3** is identified. For example, see: (a) Shi, M.; Jiang, J. K.; Feng, Y. S. *Org. Lett.* **2000**, *2*, 2397. (b) Shi, M.; Jiang, J. K. *Tetrahedron* **2000**, *56*, 4793. (c) Shi, M.; Jiang, J. K.; Cui, S. C.; Feng, Y. S. *J. Chem. Soc., Perkin Trans.* **2001**, *1*, 390. (d) Shi, M.; Feng, Y.-F. *J. Org. Chem.* **2001**, *66*, 406. (e) Shi, M.; Jiang, J. K.; Cui, S. C. *Tetrahedron* **2001**, *57*, 7343.7.
(14) Kataoka, T.; Kinoshita, H.; Iwama, T.; Tsujiyama, S.-I.; Iwamura, T.; Watanabe, S.-I.; Muraoka, O.; Tanabe, G. *Tetrahedron* **2000**, *56*, 4725.

$TiCl_4$-promoted protocol could offer an effective route to access asymmetric versions of BH reaction. We have decided to examine the mechanistic features of $TiCl_4$-promoted BH reaction, under base-free conditions, with the help of electronic structure calculations by using density functional theory methods. In particular, emphasis has been placed on examining the key elementary steps involved in the mechanistic course, which are compatible with the reported product distribution. The insights on whether the product distribution is guided by thermodynamic or kinetic control are sought. Several intricacies involved in the reaction mechanism are unraveled and the results are presented in the following sections.

Computational Details

All calculations were performed with Gaussian03 quantum chemical program.[15] Full geometry optimizations followed by frequency calculations on the stationary points were carried out to ascertain the nature of the stationary points as minima or first-order saddle points on the respective potential energy surfaces. We have employed Los Alamos pseudopotential basis set (LANL2DZ)[16] for titanium and hybrid density functionals mPW1K[17] and B3LYP[18] in combination with 6-31+G** basis set for all other atoms.[19] All transition states were characterized by one and only one imaginary frequency pertaining to the desired reaction coordinate. The intrinsic reaction coordinate (IRC) calculations were carried out at the same level of theory to further authenticate the transition states.[20] Since the reported reaction is generally conducted in less polar solvents, such as dichloromethane (ε = 8.93), the effect of solvent on the gas-phase energies is expected to be very minimal. However, in accordance with one of the referee's suggestions, we have performed geometry optimization in the condensed phase to examine the differences in energies arising as a result of the inclusion of the solvation effects on the geometries through the integral equation formalism within the polarized continuum model (IEF-PCM)[21] by using radii from the united atom topological model (UAKS). The level of theory employed is IEF-PCM(CH_2Cl_2)/mPW1K/6-31+G**,LANL2DZ//mPW1K/6-31+G**,LANL2DZ for this purpose. It is found that the changes in the relative energies are only marginal, as expected. The energies reported herein include zero-point vibrational energy (ZPVE) correction on the "bottom-of-the-well" values. The relative energies calculated using the B3LYP functional, in general, are found to be higher than those obtained by using the mPW1K functional. The B3LYP data is provided only in Supporting Information. The qualitative agreement between the results obtained using both these functionals are found to be the same.

Results and Discussion

The mechanism of $TiCl_4$-promoted BH reaction between MVK and acetaldehyde is examined by identifying all key intermediates, transition states, and reactants using the density functional theory methods. The reaction can broadly be viewed as consisting of the generation of an enolate intermediate and the C−C bond formation. Various mechanistic possibilities primarily differing in the coordination of the carbonyl compounds with $TiCl_4$ are considered.[22] Reactions involving mononuclear titanium complexes with one molecule each of MVK and aldehyde are examined in detail.

The first key step in $TiCl_4$-promoted BH reaction is the generation of enolate **3a** by a chloride transfer reaction as shown in Scheme 2. Although we have considered both *s-cis* and *s-trans* conformers of MVK, the discussion on *s-cis*-MVK (represented as *cis*-MVK in the text) is presented first. Multiple possibilities involving intermediates **1a** and **1b** are considered, wherein $TiCl_4$ coordinates, respectively, with acetaldehyde and MVK.[23] The intermediate **1b**, where MVK is bound to the titanium, can undergo a chloride transfer involving a cyclic six-membered transition state, **TS(1b−2b)**, resulting in a chloro enolate **2b**. The optimized geometry of **TS(1b−2b)** as given in Figure 1 exhibits a distorted trigonal bipyramidal topology around the titanium center. The chloro enolate **2b** can then bind with a molecule of acetaldehyde to furnish titanium enolate **3a** with a penta-coordinate arrangement of the ligands. The generation of **3a** through another pathway where both MVK and acetaldehyde are bound to $TiCl_4$ (**2a**), prior to the chloride transfer, is also examined. Two key isomers of **2a** on the basis of the relative dispositions between MVK and acetaldehyde, as either axial−axial ($\mathbf{2a_{aa}}$) or axial−equatorial ($\mathbf{2a_{ae}}$), are considered.[24] Akin to **2a**, three isomers of **3a** such as $\mathbf{3a_{aa}}$, $\mathbf{3a_{ae}}$, and $\mathbf{3a_{ea}}$ are considered as well.[25] In these notations, the first subscript refers to the coordination of acetaldehyde while the second relates to the position of MVK.

Different geometric possibilities for **2a** to **3a** conversion arising as a result of the differences in the coordination patterns of MVK and acetaldehyde are readily evident. The intermediate $\mathbf{2a_{aa}}$ can undergo a chloride transfer through **TS**($\mathbf{2a_{aa}}$−$\mathbf{3a_{aa}}$) to yield enolate $\mathbf{3a_{aa}}$. However, in the case of $\mathbf{2a_{ae}}$ two kinds of chloride transfers to MVK are possible. Either the axial or the equatorial chloride, with respect to the acetaldehyde, can be transferred. The notations $\mathbf{TS_e}$ and $\mathbf{TS_a}$ denote, respectively, the transfer of equatorial and axial chloride to MVK, where e and a are defined with respect to the position of acetaldehyde.

(15) Frisch, M. J. et al. *Gaussian 03*, revision C.02; Gaussian, Inc.: Wallingford CT, 2004. (See Supporting Information for full citation).

(16) (a) Hay, P. J.; Wadt, W. R. *J. Chem. Phys.* **1985**, *82*, 270. (b) Hay, P. J.; Wadt, W. R. *J. Chem. Phys.* **1985**, *82*, 299. (c) *Methods of Electronic Structure Theory*; Dunning, T. H., Jr., Hay, P. J., Schaeffer, H. F., III, Eds.; Plenum Press: New York, 1977.

(17) (a) Lynch, B. J.; Fast, P. L.; Harris, M.; Truhlar, D. G. *J. Phys. Chem. A* **2000**, *104*, 4811. (b) Lynch, B. J.; Zhao, Y.; Truhlar, D. G. *J. Phys. Chem. A* **2003**, *107*, 1384.

(18) (a) Becke, A. D. *Phys. Rev. A* **1988**, *38*, 3098. (b) Lee, C.; Yang, W.; Parr, R. G. *Phys. Rev. B* **1988**, *37*, 785.

(19) (a) Hariharan, P. C.; Pople, J. A. *Theor. Chimica Acta* **1973**, *28*, 213. (b) Francl, M. M.; Petro, W. J.; Hehre, W. J.; Binkley, J. S.; Gordon, M. S.; De Frees, D. J.; Pople, J. A. *J. Chem. Phys.* **1982**, *77*, 3654. (c) Rassolov, V.; Pople, J. A.; Ratner, M.; Windus, T. L. *J. Chem. Phys.* **1998**, *109*, 1223.

(20) Gonzalez, C.; Schlegel, H. B. *J. Chem. Phys.* **1989**, *90*, 2154.

(21) (a) Cancès, M. T.; Mennucci, B.; Tomasi, J. *J. Chem. Phys.* **1997**, *107*, 3032. (b) Mennucci, B.; Tomasi, J. *J. Chem. Phys.* **1997**, *106*, 5151. (c) Mennucci, B.; Cancès, E.; Tomasi, J. *J. Phys. Chem. B* **1997**, *101*, 10506. (d) Tomasi, J.; Mennucci, B.; Cancès, E. *J. Mol. Str.: THEOCHEM* **1999**, *464*, 211.

(22) (a) A variety of titanium complexes of carbonyl compounds, which include both mono- and binuclear coordinations, are reported earlier in different contexts. See: Branchadell, V.; Oliva, A. *Inorg. Chem.* **1995**, *34*, 3433. (b) In this present study, we have considered only the mononuclear titanium complexes. In the case of binuclear complexes, only those complexes where the bound aldehyde and MVK are in near vicinity can undergo C−C bond-forming reaction. However, we have optimized a few representative binuclear complexes, which were found to be higher in energy than mononuclear complexes (Figure S1 in Supporting Information).

(23) The optimized geometries of **1a** and **1b** are provided in Supporting Information (Figures S2 and S3). These penta-coordinated complexes are identified to exhibit a preference toward an axial disposition of the carbonyl ligands.

(24) The difference in the gas-phase Gibbs free energies between these two conformers was found to be 3.47 kcal/mol in favor of $\mathbf{2a_{ae}}$.

(25) All the initial guess geometries for $\mathbf{3a_{ea}}$ isomer converged to $\mathbf{3a_{ae}}$ during geometry optimization.

SCHEME 2. Plausible Mechanistic Pathways for $TiCl_4$-Promoted BH reaction

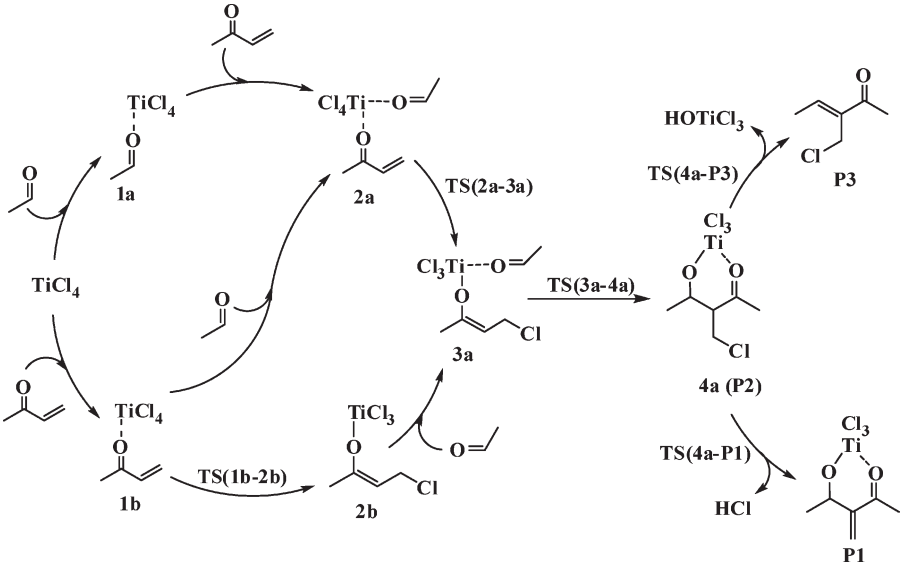

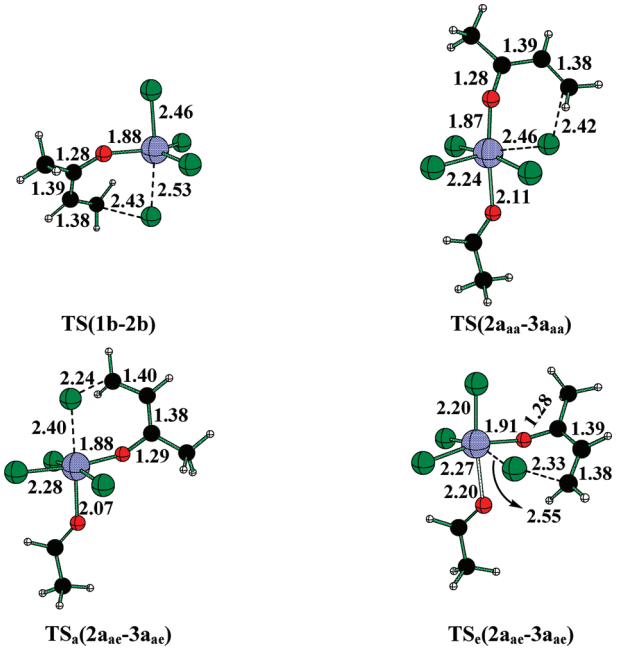

FIGURE 1. mPW1K/LANL2DZ, 6-31+G** optimized geometries of the transition states for the chloride transfer in *cis*-MVK. All bond lengths are in angstroms. Color code: green-Cl, black-C, red-O, ivory-H, light blue-Ti.

The transition state for equatorial chloride transfer **TS$_e$-(2a$_{ae}$−3a$_{ae}$)** leads to chloro enolate intermediate **3a$_{ae}$**, whereas that for the axial chloride transfer **TS$_a$(2a$_{ae}$−3a$_{ae}$)** results in another chelated complex **3a$_{ae}$′** wherein the chloride ion is loosely bound to both MVK and the titanium center. The intermediate **3a$_{ae}$′** can in turn convert to **3a$_{ae}$** through **TS(3a$_{ae}$′−3a$_{ae}$)**.[26] Both chloride transfer transition states **TS$_a$(2a$_{ae}$−3a$_{ae}$)** and **TS$_e$(2a$_{ae}$−3a$_{ae}$)** present an octahedral topology as depicted in Figure 1.

The computed relative enthalpies, as summarized in Table 1, indicate that the chloride transfer is energetically more preferred in the hexa-coordinate **2a** than that in the corresponding penta-coordinate intermediate **1b**.[27] A Michael-type addition of the chloride ion would result in increased negative charge on the oxygen atom of MVK. Thus the developing positive charge on the metal center arising due to the departure of chloride ion can be regarded as getting quenched by the developing negative charge on the bound oxygen atom of MVK.[28] In the case of intermediate **2a**, the transition states are further stabilized by the presence of the bound-aldehyde. It is also noticed that for intermediate **2a**, the transfer of equatorial chloride involving **TS$_e$-(2a$_{ae}$−3a$_{ae}$)** is kinetically more preferred. The improved stability of **TS$_e$(2a$_{ae}$−3a$_{ae}$)** can be attributed to *trans* effect as noticed commonly in substitution reactions.[29] The expulsion of chloride ion could benefit by the presence of a strong σ donor group *trans* to the leaving group. In the case of **TS$_a$(2a$_{ae}$−3a$_{ae}$)**, the ligand *trans* to the departing chloride ion is a carbonyl oxygen, which is a poorer σ-donor than a chloride ion.[30] However, in the case of **TS(2a$_{aa}$−3a$_{aa}$)** and **TS$_e$(2a$_{ae}$−3a$_{ae}$)**, the presence of another chloride ion in the *trans* position offers additional assistance to the chloride ion expulsion. This feature is evidently reflected in the relative distances of the Ti−Cl bond that undergoes scission (Figure 1). In two of the latter cases, the Ti−Cl bond is found to be slightly longer than that in **TS$_a$(2a$_{ae}$−3a$_{ae}$)**.

The discussions thus far have been confined to the *cis* conformer of MVK. It is of significance to note that the computed energy difference between the *cis* and *trans* conformers is less than 1 kcal/mol. Further, the torsional barrier for interconversion between these two conformers is found

(26) The optimized geometries of these intermediates are provided in Figure S2 in Supporting Information.

(27) It is also worth noting that the forward reaction for this step is more favored than the backward reaction.

(28) Decreased Mulliken charges are identified on titanium in **TS(1b−2b)** as compared to that in **1b** (see Table S2 in Supporting Information).

(29) Huheey, J. E.; Keiter, E. A.; Keiter, R. L. In *Inorganic Chemistry: Principles of Structure and Reactivity*; Pearson Education: Singapore, 2003.

(30) Gau, H.-M. ; Lee, C.-S.; Lin, C.-C.; Jiang, M.-K.; Ho, Y.-C.; Kuo, C.-N. *J. Am. Chem. Soc.* **1996**, *118*, 2936.

TABLE 1. Relative Energies[a] (in kcal/mol) of Stationary Points Involved in Chloride Transfer to *cis*-MVK Obtained from Gas-Phase and Solvent-Phase Optimizations Using the mPW1K Functional[b]

	gas phase			solvent phase		
	ΔE	ΔH	ΔG	ΔE	ΔH	ΔG
1b	−10.1	−9.7	1.6	−11.8	−11.4	−0.6
TS(1b−2b)	6.1	5.6	19.5	3.8	3.3	17.2
2b	−11.2	−11.3	−0.8	−10.5	−10.6	0.3
1a	−8.8	−8.7	2.6	−10.2	−10.0	1.3
$\mathbf{2a_{aa}}$	−17.7	−17.3	5.8	−20.2	−19.6	2.5
$\mathbf{TS(2a_{aa}-3a_{aa})}$	−9.3	−9.8	16.2	−10.6	−11.0	14.9
$\mathbf{3a_{aa}}$	−22.1	−22.2	0.6	−21.3	−21.4	1.4
$\mathbf{2a_{ae}}$	−20.6	−20.0	2.3	−23.1	−22.5	0.2
$\mathbf{TS(2a_{aa}-2a_{ae})}$	−4.8	−5.1	20.4	−6.1	−6.3	18.8
$\mathbf{TS_e(2a_{ae}-3a_{ae})}$	−9.4	−9.9	16.4	−11.2	−11.7	14.4
$\mathbf{3a_{ae}}$	−21.5	−21.6	1.8	−20.7	−20.8	2.7
$\mathbf{TS_a(2a_{ae}-3a_{ae})}$	−7.3	−7.9	18.5	−9.3	−9.8	16.5
$\mathbf{3a_{ae}'}$	−11.2	−11.7	14.3	−12.8	−13.2	12.5
$\mathbf{TS(3a_{ae}'-3a_{ae})}$	−7.5	−8.2	17.3	−8.6	−9.1	15.6
$\mathbf{TS(3a_{aa}-3a_{ae})}$	−14.6	−15.0	8.3	−15.0	−15.4	8.0

[a]All energies are relative to the infinitely separated reactants. [b]The LANL2DZ pseudopotential basis set was used for Ti and 6-31+G* for all other atoms. Solvent optimization was done using IEF-PCM formalism in combination with UAKS radii.

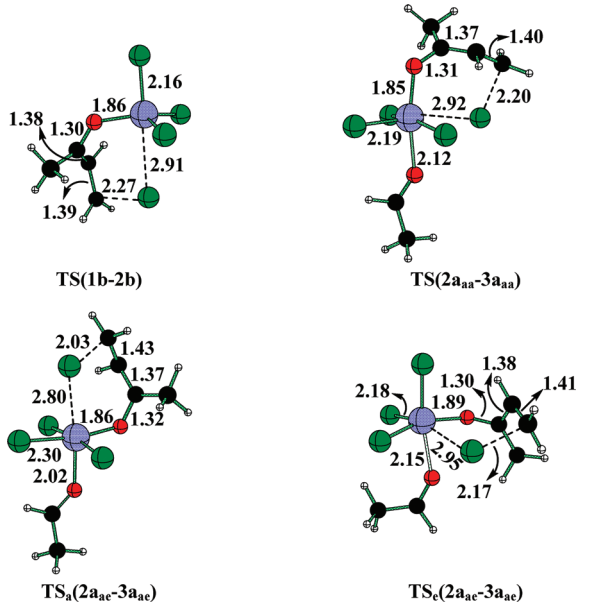

FIGURE 2. mPW1K/LANL2DZ, 6-31+G** optimized geometries of the transition states for the chloride transfer in *trans*-MVK. All bond lengths are in angstroms. Color code: green-Cl, black-C, red-O, ivory-H, light blue-Ti.

to be only about 5.8 kcal/mol in the gas phase.[31] To examine the effect of the choice of MVK conformer on the overall reaction profile, all elementary steps involving *trans*-MVK are additionally investigated. The computed relative energies of the key intermediates and transition states are provided in Table 2. The relative energies of the transition states for the chloride transfer are found to be substantially higher in *trans*-MVK as compared to the corresponding transition states in the case of *cis*-MVK. Interestingly, the energies of

(31) (a) Under the normal experimental conditions, the cis and trans conformers could easily co-exist in equilibrium with a surmountable barrier for interconversion. (b) The optimized geometries of TSs corresponding to *cis*−*trans* interconversion are given in Figure S4, and their energies at the mPW1K/6-31+G** level of theory are summarized in Table S2 in Supporting Information.

TABLE 2. Relative Energies[a] (in kcal/mol) of Stationary Points Involved in Chloride Transfer to *trans*-MVK Obtained from Gas-Phase and Solvent-Phase Optimizations Using the mPW1K Functional[b]

	gas phase			solvent phase		
stationary point	ΔE	ΔH	ΔG	ΔE	ΔH	ΔG
1b	−9.1	−8.8	2.8	−11.1	−10.8	0.6
TS(1b−2b)	27.2	26.7	40.6	26.2	25.8	39.4
2b	−10.0	−10.0	−0.5	−9.6	−9.7	0.5
1a	−8.8	−8.7	2.6	−10.2	−10.0	1.3
$\mathbf{2a_{aa}}$	−16.4	−16.1	7.6	−19.2	−18.8	4.7
$\mathbf{TS(2a_{aa}-3a_{aa})}$	14.3	13.9	39.6	13.7	13.4	38.9
$\mathbf{3a_{aa}}$	−20.5	−20.5	1.1	−20.0	−20.0	1.8
$\mathbf{2a_{ae}}$	−20.5	−20.1	3.4	−22.8	−22.2	0.3
$\mathbf{TS(2a_{aa}-2a_{ae})}$	−4.1	−4.4	21.3	−5.5	−5.9	19.8
$\mathbf{TS_e(2a_{ae}-3a_{ae})}$	17.9	17.4	43.7	15.9	15.4	41.4
$\mathbf{TS_a(2a_{ae}-3a_{ae})}$	23.5	22.9	49.2	21.4	20.9	46.9
$\mathbf{3a_{ae}}$	−19.1	−19.0	2.8	−19.2	−19.1	2.9
$\mathbf{TS(3a_{aa}-3a_{ae})}$	−12.5	−12.9	9.5	[c]	[c]	[c]

[a]All energies are relative to the infinitely separated reactants. [b]The LANL2DZ pseudopotential basis set was used for Ti and 6-31+G* for all other atoms. Solvent optimization was done using IEF-PCM formalism in combination with UAKS radii. [c]The stationary point could not be located in the condensed phase calculation.

the titanium···MVK prereacting complex (**1b**) for both *cis* and *trans* MVK are very similar. Such large differences in the barriers for the chloride transfer can therefore be ascribed to the differences in the geometric features of the transition states. In the case of *trans*-MVK, two prominent features are evident from the optimized geometries as given in Figure 2. These include (a) larger geometric distortion of the α-carbon of MVK associated with the C−Cl bond formation contributing to changes in the reaction coordinate and (b) a longer Ti−Cl bond implying a late transition state.[32] The α-carbon is identified to suffer greater geometric distortion in the chloride transfer step, which could directly affect the efficiency of delocalization in the MVK backbone involving the carbonyl group.[33] Both of these factors will render a greater positive charge on the metal center in the case of *trans*-MVK.[34]

As in the case of *cis*-MVK, the transfer of equatorial chloride in the hexa-coordinate intermediates ($\mathbf{2a_{aa}}$ and $\mathbf{2a_{ae}}$) is found to be energetically more favorable than in the corresponding penta-coordinate intermediate (**1b**). The key difference with *cis*-MVK pertains to the relative stability of **TS(1b−2b)** as compared to $\mathbf{TS_a(2a_{ae}-3a_{ae})}$ for the chloride transfer.[35] In *cis*-MVK, $\mathbf{TS_a(2a_{ae}-3a_{ae})}$ is more preferred than **TS(1b−2b)**. Also the transfer of chloride ion axial to acetaldehyde does not yield a chelated complex similar to $\mathbf{3a_{ae}'}$ as noticed in the case of *cis*-MVK. The intermediates $\mathbf{2a_{aa}}$, $\mathbf{2a_{ae}}$ and $\mathbf{3a_{aa}}$, $\mathbf{3a_{ae}}$ can convert to each other respectively *via* a turnstile and Berry pseudorotation. For instance, the transition state $\mathbf{TS(2a_{aa}-2a_{ae})}$ for the conversion

(32) Higher positive charge on titanium is noticed in the case of *trans*-MVK as compared to that in *cis*-MVK. (see Table S1 in Supporting Information).

(33) We have calculated extent of pyramidalization of the α-carbon involved in the chloride transfer step as defined by Radhakrishnan, T. P.; Agranat, I. *Struct. Chem.* **1990**, *2*, 107. The calculated extent of polarization is provided in Table S3 in Supporting Information.

(34) This is partly evident from the computed Mulliken charges on titanium and oxygen atom of MVK in the corresponding TSs of the two cases (see Table S1 in Supporting Information).

(35) Another key difference for chloride transfer step in *trans*-MVK is that only **TS(1b−2b)** and $\mathbf{TS(2a_{aa}-3a_{aa})}$ favor the forward reaction. For $\mathbf{TS_e(2a_{ae}-3a_{ae})}$ and $\mathbf{TS_a(2a_{ae}-3a_{ae})}$ both forward and backward reaction are found to be equally favored.

of $\mathbf{2a_{aa}}$ to $\mathbf{2a_{ae}}$, which corresponds to a turnstile mechanism for exchange of axial/equatorial positions for hexacoordinated intermediate, is identified.[36]

The next step after the generation of titanium enolate (**3a**) is an intramolecular aldol reaction with acetaldehyde. In principle, the enolate can attack either of the prochiral faces offered by acetaldehyde (*vide infra*). The obvious geometric requirement for this C−C bond formation is the proximity between the nucleophile and the electrophile. It is therefore important that intermediate **3a** maintains an axial−equatorial geometric relationship between the titanium-bound enolate and acetaldehyde. The intermediate $\mathbf{3a_{aa}}$ should therefore convert to $\mathbf{3a_{ae}}$, which in turn will serve as a reactive configuration. A low energy transition state responsible for this conversion through Berry's pseudorotation **TS**($\mathbf{3a_{aa}}$−$\mathbf{3a_{ae}}$) is identified.[37]

In general, the stereochemical outcome of aldol reactions of the type similar to the present case are qualitatively explained using the Evans or Zimmerman−Traxler transition state models. These models rely on the relative energies of cyclic chelated transition state structures either in chair or boat geometry. However, the topology around the metal is often paid less attention.[38,39] In an earlier study, the observed diastereoselectivity in an aldol reaction between titanium-(*Z*)-enolate and a α-CF_3 containing ketone has been rationalized on the basis of weak Ti···F interactions.[40] Along the similar lines, we reasoned that the interaction between the α-CH_2Cl group and the titanium could perhaps influence the preferred stereochemical mode of addition. Indeed, transition states with a square bipyramidal topology around the titanium, with two equatorial oxygens and a weakly coordinating chlorine from the axial α-CH_2Cl group, is identified. The optimized geometries of these transition states are provided in Figure 3. Additional transition state geometries devoid of such interactions are also examined. The consideration of all these possibilities led to transition states with a penta-coordinated trigonal bipyramidal topology around the titanium.[41] Both axial−equatorial (ae) and equatorial−axial (ea) dispositions of the aldehyde and the enolate are considered.[42] Further, the *si*−*re* as well as *re*−*re* modes of additions between the prochiral faces of the aldehyde and the enolate, respectively, involved in the bond formation are also examined.

The approach between the aldehyde and the enolate in the *si*−*si* stereochemical mode would lead to a product with a *syn* configuration ($\mathbf{4a_{syn}}$) of the substituents around the developing C−C bond. The *si*−*re* approach on the other hand results in $\mathbf{4a_{anti}}$.[43] Some interesting geometric features became evident from the analyses of the optimized TS geometries as provided in Figure 3.[44] In the square bipyramidal topology, only a boat-like transition state for the C−C bond formation is identified as the preferred geometry. However, in trigonal bipyramidal case, both boat-like and chair-like geometries are identified. It is further found that the boat-like geometry leading to the *anti* diastereomer is energetically more preferred over the corresponding chair-like geometry responsible for the *syn* product.

The relative energies of various TSs for the C−C bond formation involving *cis*-MVK are provided in Table 3. A general preference toward the formation of *anti* diastereomer is noticed. Interestingly, the lower energy six-membered

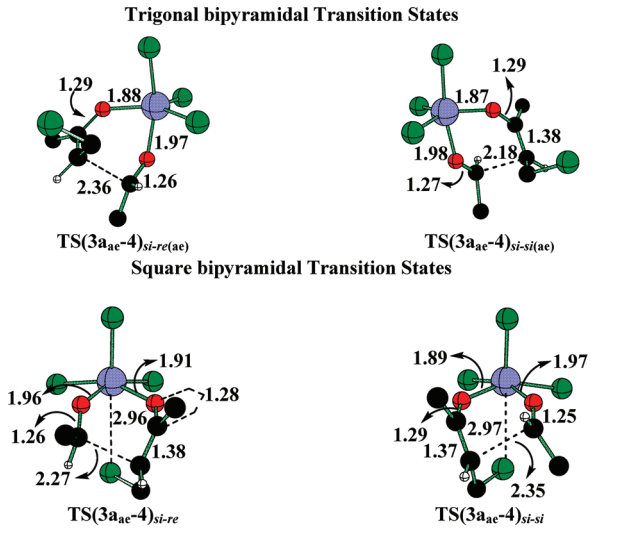

FIGURE 3. mPW1K/LANL2DZ, 6-31+G** optimized geometries of the transition states for C−C bond formation step for *cis*-MVK. All bond lengths are in angstroms. Hydrogen atoms on methyl groups have been removed for clarity. Color code: green-Cl, black-C, red-O, ivory-H, light blue-Ti.

TABLE 3. Relative Energies[a] (in kcal/mol) of the Stationary Points Involved in the C−C Bond-Formation for *cis*-MVK Obtained from Gas Phase and Solvent Phase Optimizations Using the mPW1K Functional[b]

	gas phase			solvent phase		
stationary point	Δ*E*	Δ*H*	Δ*G*	Δ*E*	Δ*H*	Δ*G*
Trigonal Bipyramidal Topology						
TS($\mathbf{3a_{ae}}$−**4**)$_{si-re}$	−8.9	−10.1	17.1	−9.6	−10.8	16.0
TS($\mathbf{3a_{ae}}$−**4**)$_{re-re}$	−6.7	−8.0	19.1	−7.7	−8.9	17.7
Square Bipyramidal Topology with Ti···Cl Interaction						
TS($\mathbf{3a_{ae}}$−**4**)$_{si-re}$	−5.7	−7.1	21.4	−8.8	−10.2	18.4
TS($\mathbf{3a_{ae}}$−**4**)$_{re-re}$	−2.4	−3.7	24.6	−5.7	−7.0	21.5
$\mathbf{4a_{anti}}$	−38.9	−40.2	−12.5	−40.2	−41.5	−13.8
$\mathbf{4a_{syn}}$	−36.1	−37.4	−10.1	−37.7	−39.1	−11.6

[a]All energies are relative to the infinitely separated reactants. [b]The LANL2DZ pseudopotential basis set was used for Ti and 6-31+G* for all other atoms. Solvent optimization was done using IEF-PCM formalism in combination with UAKS radii.

(36) (a) The details of the corresponding transition state **TS**($\mathbf{3a_{aa}}$−$\mathbf{3a_{ae}}$) for the conversion of $\mathbf{3a_{aa}}$ to $\mathbf{3a_{ae}}$ are provided in Supporting Information (Figure S2). (b) An interesting discussion on similar situations can be found in (i) Cass, M. E.; Hib, K. K.; Rzepa, H. S. *J. Chem. Educ.* **2006**, *83*, 336 and (ii) http://www.ch.ic.ac.uk/rzepa/bpr/ (accessed on August 3, 2009).

(37) The optimized transition state geometry is provided in Figure S2 in Supporting Information.

(38) Nakamura, E.; Kuwajima, I. *Tetrahedron Lett.* **1983**, *24*, 3343.

(39) Mahrwald, R. *Chem. Rev.* **1999**, *99*, 1095.

(40) Itoh, Y.; Yamanaka, M.; Mikami, K. *J. Am. Chem. Soc.* **2004**, *126*, 13174.

(41) However, all initial guess geometries for **TS**($\mathbf{3a_{ea}}$−**4**)$_{si-re(ea)}$ and **TS**($\mathbf{3a_{ea}}$−**4**)$_{re-si(ea)}$ converged to **TS**($\mathbf{3a_{ea}}$−**4**)$_{si-re(ae)}$ and **TS**($\mathbf{3a_{ea}}$−**4**)$_{re-si(ae)}$, respectively, during the course of geometry optimization.

(42) The "ea" possibility was found only at the B3LYP gas-phase calculation.

(43) An illustration of how these diastereomeric transition states would lead to *syn* and *anti* product is provided in Figure S5 in Supporting Information.

(44) Additional possibilities involving *re*−*re* as well as *re*−*si* modes of approaches between the aldehyde and the enolate is examined. These TSs leading to diastereomeric products are provided in Figure S6 in Supporting Information.

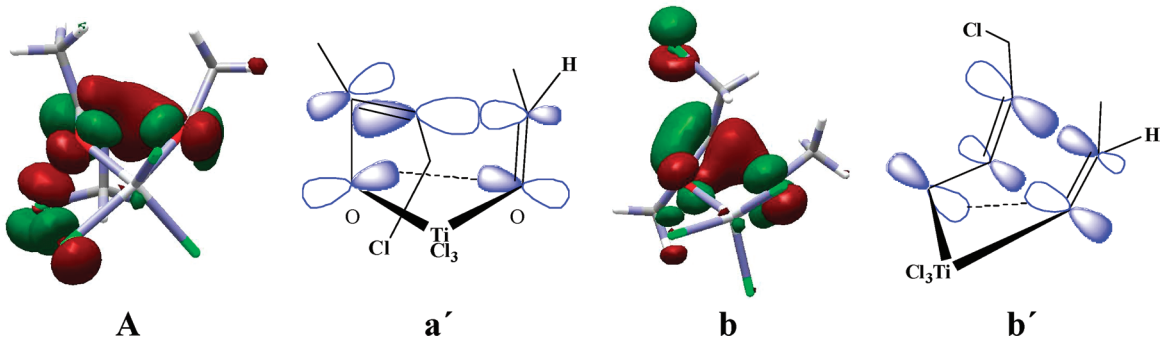

FIGURE 4. Illustration of favorable secondary orbital interaction in the C−C bond formation transition states. **a** and **b** are the highest occupied Kohn−Sham orbital contours (isodensity = 0.05) for *si*−*re* and *si*−*si* modes, respectively. **a**′ and **b**′ represent a simplified qualitative depiction of these interactions.

boat-like TSs are consistent with the TSs proposed for Ti mediated aldol reaction.[37] It is further evident that among the TSs exhibiting weak Ti···Cl interaction, such as in the square bipyramidal **TS(3a$_{ae}$−4)**$_{si-re}$, the ones that lead to *anti* product are found to be energetically more favorable.[45] This implies that the Ti···Cl weak interaction does not have any direct effect in determining the diastereoselectivity. Although product **4a** is not isolated in $TiCl_4$-mediated BH reaction under the normal experimental conditions, it is worth pointing out that a product similar to **4a** with an *anti* configuration has been reported when α,β unsaturated *N*-benzoxazolinone is employed as a substrate.[11b] The relative preference toward a boat-like TS geometry had earlier been attributed to the reduced steric hindrance between α-Me of MVK and substituents on aldehyde as compared to that present in the corresponding chair arrangement.[14] However, in the present case, such effects are expected to be minimal as the methyl group of the aldehyde is relatively smaller. In the case of square bipyramidal topology, all TSs present a boat-like geometry, which are found to be adequate toward explaining the *syn*/*anti* preference. In order to identify any additional contributing factors that could influence the diastereoselectivity, Kohn−Sham orbitals of the key transition states are carefully examined.

In the most preferred C−C bond formation transition state (**3a$_{ae}$−4**)$_{si-re}$ leading to *anti* diastereomer, the highest occupied Kohn−Sham orbital is found to involve contributions from oxygen atom and π orbital of enolate as well as π* orbital of the aldehyde. Interestingly, in all the TSs the aldehyde and enolate oxygens are favorably oriented to promote effective orbital interaction. In the TSs leading to *syn* diastereomer, the oxygen centered orbitals are aligned to develop only a lateral interaction while that corresponding to *anti* diastereomer a more stabilizing head-on interaction is identified (Figure 4).[46]

In the case of *trans*-MVK the *E* configuration of enolate is considered. Unlike in *cis*-MVK, the α-CH_2Cl group here is away from Ti to develop any Ti···Cl interaction due to the inherent geometric constraints. The TSs similar to the square bipyramidal topology as with *cis*-MVK are therefore not possible in the present case. The geometries of all transition

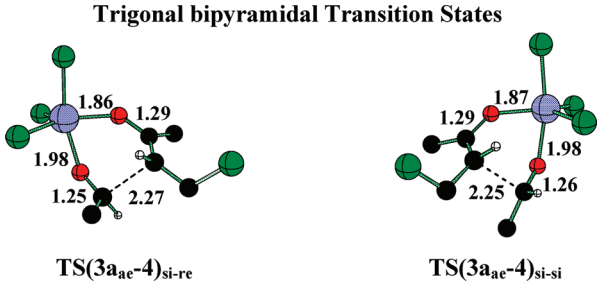

FIGURE 5. mPW1K/LANL2DZ, 6-31+G** optimized geometries of the transition states for the C−C bond formation step for *trans*-MVK. All bond lengths are in angstroms. Only select hydrogens are shown. Color code: green-Cl, black-C, red-O, ivory-H, light blue-Ti.

states involved in the case of *trans*-MVK are found to maintain a cyclic boat-like structure (Figure 5).

The summary of the computed relative energies for the C−C bond formation TSs in the case of *trans*-MVK are provided in Table 4. It can be readily noted that the *re*−*re* mode of addition leading to the *syn* diastereomer is more favorable, as opposed to the preferred *anti* diastereomer predicted for *cis*-MVK.[47]

The formation of two diasteromers of **4a**, resulting from the approaches between the prochiral faces of the enolate and acetaldehyde is considered. As noted earlier, the *si*−*re* mode of addition through **TS(3a$_{ae}$−4)**$_{si-re}$ will lead to **4a$_{anti}$** product, whereas the *si*−*si* through **TS(3a$_{ae}$−4)**$_{si-si}$ results in **4a$_{syn}$** diastereomer. The **4a$_{anti}$** and **4a$_{syn}$** diastereomers, from both *cis* and *trans* MVK are conformational isomers. We have also located the transition state connecting these conformers. For instance, the barrier for the conversion of **4a$_{anti}$** obtained from *cis*-MVK to the corresponding **4a$_{anti}$** product arising from *trans*-MVK is found to be 6.81 kcal/mol in the gas phase. It is identified that the product **4a** generated from *cis*-MVK presents an *endo* orientation of the α-CH_2Cl group with respect to the chelated ring, whereas in the corresponding *trans*-MVK it gives rise to an *exo* disposition. The *endo*/*exo* geometric arrangement of the α-CH_2Cl group is illustrated with the help of **4a$_{anti}$** as a representative product in Figure 6. The *endo* isomer of **4a$_{anti}$**

(45) The forward reaction is found be more favorable in both cases.

(46) The Kohn−Sham orbital contours of important frontier orbitals for all key TSs are provided in Figure S7 of Supporting Information.

(47) This is in agreement with an earlier report on the aldol reaction of trichlorotitanium enolates of cyclohexanones, where a *syn* product has been identified. The forward reaction was found to be more favored as in the case of *cis*-MVK.

TABLE 4. Relative Energies[a] (in kcal/mol) of Stationary Points Involved in C−C Bond-Formation for *trans*-MVK Obtained from Gas-Phase and Solvent-Phase Optimizations Using the mPW1K Functional[b]

	gas phase			solvent phase		
stationary point	ΔE	ΔH	ΔG	ΔE	ΔH	ΔG
TS(3a$_{ae}$−4)$_{si-re}$	−6.8	−7.9	18.3	−7.9	−9.0	17.1
TS(3a$_{ae}$−4)$_{re-re}$	−9.7	−10.9	16.1	−10.5	−11.7	15.1
4a$_{anti}$	−35.4	−36.6	−10.2	−36.7	−38.0	−10.7
4a$_{syn}$	−36.4	−37.7	−10.5	−37.9	−39.2	−11.8

[a]All energies are relative to the infinitely separated reactants. [b]The LANL2DZ pseudopotential basis set was used for Ti and 6-31+G* for all other atoms. Solvent optimization was done using IEF-PCM formalism in combination with UAKS radii.

4a$_{anti}$ from *cis*-MVK **4a$_{anti}$** from *trans*-MVK

FIGURE 6. mPW1K/LANL2DZ, 6-31+G** optimized geometries of **4a$_{anti}$** intermediates formed from *cis* and *trans* MVK. All bond lengths are in angstroms. Hydrogen atoms on methyl groups are not shown for sake of clarity.

is found to be slightly more stable as compared to the *exo* arrangement (Tables 3 and 4).

Once the diastereomers of **4a** are available, the ensuing elimination of suitable small molecules would furnish the BH product, as described earlier in Scheme 2. In the last stage of the mechanistic scheme, the expulsion of HCl from **4a** can lead to the $TiCl_3$-bound **P1**, whereas the removal of $HOTiCl_3$ results in **P3**. The optimized geometries of these key transition states are provided in Figure 7. The formation of **P3** demands a *syn* elimination of $HOTiCl_3$ from **4a**. In order for this elimination to take place, **4a** should undergo a rotation along the newly formed C−C single bond toward a *syn* periplanar arrangement between the leaving groups. In the unchelated conformer of **4a$_{syn/anti}$**, referred as **4a1$_{syn/anti}$**, the -$OTiCl_3$ moiety and the hydrogen α to the carbonyl group are *gauche* to each other. It is worth noting here that **4a1$_{syn}$** upon *syn* elimination will yield the *E* isomer of **P3(*E*)**, whereas **4a1$_{anti}$** will give the *Z* isomer **P3(*Z*)**. The elimination TSs relating the corresponding conformers with their respective products are **TS1(4a1$_{syn}$−P3(*E*))** and **TS1(4a1$_{anti}$−P3(*Z*))**. The structural features of the lower energy TSs convey that the carbonyl group tends to remain in conjugation with the developing C=C double bond. The additional transition states for the above two cases, wherein the carbonyl group remains nonplanar with respect to the incipient double bond, are found to be about ∼3 kcal/mol higher in energy in the gas phase.[48] The normal BH product **P1** (with a bound $TiCl_3$ moiety) can directly be obtained from **4a$_{syn/anti}$**, generated either from *cis* or *trans* MVK, by the elimination of HCl. The optimized geometries of the corresponding transition states **TS(4a$_{syn}$−P1)** and **TS(4a$_{anti}$−P1)** are provided in Figure 7. The difference in geometries of **TS(4a$_{syn}$−P1)** arising from both *cis* and *trans* MVK is primarily with the conformation of the chelated ring.

(48) See Table S6 and Figure S8 in Supporting Information for additional details on the energies and optimized geometries, respectively.

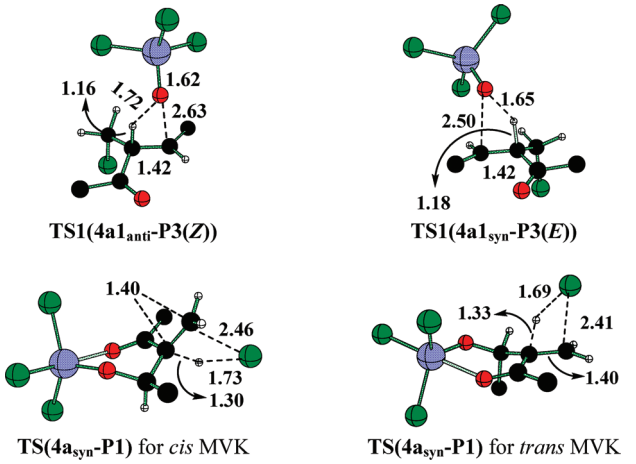

TS1(4a1$_{anti}$-P3(*Z*)) **TS1(4a1$_{syn}$-P3(*E*))**

TS(4a$_{syn}$-P1) for *cis* MVK **TS(4a$_{syn}$-P1)** for *trans* MVK

FIGURE 7. mPW1K/LANL2DZ, 6-31+G** optimized geometries of the transition states for the formation **P3(*Z*/*E*)** and **P1**. All bond lengths are in angstroms. Hydrogen atoms on methyl groups have been removed for clarity. Color code: green-Cl, black-C, red-O, ivory-H, light blue-Ti.

The energetic details of various TSs and intermediates associated with the formation of **P1** and **P3** are summarized in Table 5. The computed Gibbs free energies of the transition states reveal that the formation of *Z* diastereomer is slightly more preferred over the *E* isomer, which is in agreement with the experimental observations. On the basis of the geometric features of these two TSs, it appears that increasing the size of the aldehyde could help modulate the energy separation between the TSs leading to *E* or *Z* isomers. With larger or bulkier aryl groups, the TSs for the formation of **P3(*E*)** might get relatively more destabilized as a result of steric effects.

One of the most important trends emerging from the computed relative energies is that the pathways leading to **P3** are kinetically more favorable than those leading to **P1**.[49] If the *gauche* conformer of **4a1** is destabilized, then the formation of product **P1** could well become more feasible. This factor could possibly be operating in the case of cyclohexenones, which are known to furnish **P1**, where the rotation of the carbonyl and -CH_2Cl moiety is restricted. At the same time, with substituted MVKs **P3(*Z*)** is observed as the major product as opposed to **P1** for cyclohexenones.[12] To confirm this hypothesis, we have located the TSs corresponding to the expulsion of $HOTiCl_3$ and HCl from the intermediates equivalent to **4a1** and **4a**, in the BH reaction between acetaldehyde and cyclohex-2-enone. The computed data indeed suggests that the formation of **P1** is kinetically more feasible than **P3** by about 4 kcal/mol in the gas phase.

It can be readily noticed that the present reaction sequence involves several steps wherein association and dissociation of reagents take place. The effect of entropy in the computed energetics is therefore expected to be vital. To examine the significance of the entropy changes (ΔS) associated with the

(49) For the expulsion of $HOTiCl_3$ and HCl it appears that the backward reaction is more favored; however, we would like to note that the products **P3** and **P1** considered here have weakly bound $HOTiCl_3$ and HCl, respectively. This will lead to an underestimation of the translational entropy upon product formation. If translational freedom of independent molecules is considered, the barrier heights could be higher for the backward reaction.

TABLE 5. Relative Energies[a] (in kcal/mol) of the Stationary Points Involved in formation P3 and P1 Obtained from Gas Phase and Solvent Phase Optimizations Using the mPW1K Functional[b]

	gas phase			solvent phase		
	ΔE	ΔH	ΔG	ΔE	ΔH	ΔG
TS4a$_{anti}$	−32.7	−34.5	−5.7	−33.2	−35.0	−6.4
TS4a$_{syn}$	−28.9	−30.9	−1.9	−30.5	−32.4	−3.5
4a1$_{anti}$	−34.1	−34.9	−10.8	−32.5	−33.3	−8.7
TS1(4a1$_{anti}$−P3(*Z*))	12.1	11.5	35.7	9.9	9.4	33.4
P3(*Z*)[c]	−28.2	−28.4	−6.9	−27.0	−27.2	−5.1
4a1$_{syn}$	−30.2	−31.5	−6.0	−32.7	−33.5	−9.0
TS1(4a1$_{syn}$−P3(*E*))	13.8	13.4	37.0	[e]	[e]	[e]
P3(*E*)[c]	−17.5	−17.4	2.4	−15.5	−15.3	5.5
			cis-MVK			
TS(4a$_{anti}$−P1)	19.1	18.1	44.8	16.5	15.5	42.4
TS(4a$_{syn}$−P1)	19.2	18.1	44.9	17.2	16.1	43.0
			trans-MVK			
TS(4a$_{anti}$−P1)	20.3	19.1	46.1	16.8	15.7	42.4
TS(4a$_{syn}$−P1)	19.5	18.4	45.4	15.8	14.7	41.6
P1[d]	−22.8	−22.7	0.1	−24.2	−24.0	−2.3

[a]All energies are relative to the infinitely separated reactants. [b]The LANL2DZ pseudopotential basis set was used for Ti and 6-31+G* for all other atoms. Solvent optimization was done using IEF-PCM formalism in combination with UAKS radii. [c]Corresponds to $HOTiCl_3$ bound **P3**. [d]Corresponds to $TiCl_3$ bound **P1** with HCl hydrogen bonded to it. [e]The stationary point could not be located in the condensed phase calculation.

binding of ligands with the Lewis acid, we have analyzed the changes in the translational, rotational, and vibrational entropies in various elementary steps. The computed values indicate, with striking consistency between various steps, that the loss of translational entropy is the major contributing factor toward the ΔS.[50]

Another interesting observation obtained from the present study relates to the role of solvation effects toward the computed energetics. As mentioned in the earlier sections that the experiments have been known, for the substrates under investigation here, in relatively less polar solvents, such as DCM (CH_2Cl_2). In an effort to ascertain the effect of continuum dielectric on the geometries and the accompanying energy changes, we have compared the results obtained through the gas-phase and solvent-phase geometry optimizations. A graphical summary depicting the impressively close agreement between these two approaches is provided in Figure S9 - S13 in the Supporting Information. On the basis of this analysis, we propose that role of DCM solvent on the mechanism of $TiCl_4$-promoted BH reaction as reported in this work is only peripheral. It further endorses the view that the full geometry optimizations are not quite necessary for modeling reactions conducted under relatively low polarity solvents as well as for those which does not involve well-developed charges or zwitterionic species in the reaction course. A few additional and pertinent details emerged from this analysis is that the inclusion of solvent effects through full geometry optimization brings about a consistent, though marginal, stabilization of almost all stationary points. The results obtained from the gas-phase calculations are found to be in good agreement with those obtained from solvent-phase calculations.

(50) The total entropy can be partitioned into electronic, translational, rotational, and vibrational contributions. The ΔS term, in the equation $\Delta G = \Delta H - T(\Delta S)$, can be calculated with respect to the infinitely separated reactants. This will yield the expression: $\Delta G = \Delta H - T(\Delta S_{trans}) - T(\Delta S_{rot}) - T(\Delta S_{vib})$. Here, electronic contribution does not appear in the equation as only the ground state configuration is considered. A comprehensive list of $T(\Delta S_{trans})$, $T(\Delta S_{rot})$, and $T(\Delta S_{vib})$ terms are provided in Tables S7−S11 in Supporting Information. The relative changes in the translational and rotational entropy, $\Delta S_{translational}$ and $\Delta S_{rotational}$, respectively, are found to be negative, and the corresponding changes in vibrational entropy ($\Delta S_{vibrational}$) is positive. Moreover, the magnitude of $\Delta S_{rotational}$ is nearly half that of $\Delta S_{translational}$. The $\Delta S_{vibrational}$ is found to be only slightly less than that of $\Delta S_{rotational}$. As a result, $\Delta S_{rotational}$ and $\Delta S_{vibrational}$ can be taken as nullifying each other. This situation suggests that the entropy effect is almost entirely due to $\Delta S_{translational}$.

Conclusion

The $TiCl_4$-promoted Baylis−Hillman reaction between methyl vinyl ketone and acetaldehyde, under base-free conditions, has been investigated using the density functional theories. Different mechanistic scenarios have been examined with an emphasis on the coordination topology around the Ti(IV) center. The three key steps in the reaction have been identified as (i) the generation of the titanium-bound chloro enolate intermediate, (ii) the C−C bond formation between the enolate and acetaldehyde, and (iii) the expulsion of either HCl or $HOTiCl_3$ to furnish BH products.

The computed energetics for the key chloride transfer step reveal that the reaction of *s-cis* conformer of MVK is kinetically more favored over the *s-trans* conformer. A hexa-coordinate topology (**2a$_{aa}$**) has been found to be more preferred over the corresponding penta-coordinate arrangement in the chloride transfer step for both *cis* and *trans* MVK. The resulting *Z*-enolate from *cis*-MVK has been found to favor *anti* diastereoselectivity in the C−C bond formation step, whereas *syn* selectivity has been predicted for the *E*-enolate derived from *trans*-MVK. Frontier orbital interactions between the oxygen atoms of aldehyde and enolate in the concerned TSs have been identified as one of the factors contributing toward the predicted diastereoselectivity. Among the experimentally observed products in $TiCl_4$-promoted BH reaction involving MVK, viz., **P3(*Z*)** and **P1**, our results predict that the formation of **P3(*Z*)** is evidently favored over **P1** under the base-free conditions. However, the product **P1** is predicted to be energetically more favored when cyclohexenone is employed as the Michael acceptor (and ensuing generation of the enolate). These predictions are in agreement with the observed experimental reports wherein product **P3(Z)** was observed with substituted MVKs, whereas **P1** was the major product with cyclohexenones.

Acknowledgment. Generous computing time from the IIT Bombay computer center is acknowledged. R.B.S. acknowledges research grant 07YIA001 from Industrial Research and Consultancy Center (IRCC)-IIT Bombay through the young investigator award scheme. C.P. acknowledges a junior research fellowship from the Department of Science and Technology, New Delhi through SR/S1/PC-39/2005.

Supporting Information Available: Optimized Cartesian coordinates, energy and geometry of various intermediates/transition states, complete citation for ref 15, and other pertinent details. This material is available free of charge via the Internet at http://pubs.acs.org.